Evaporation of water/ethanol droplets in an air flow: experimental study and modelling

E.M. Starinskaya[1], N.B. Miskiv[1,2], A.D. Nazarov[1,2], V.V. Terekhov[1,2], V.I. Terekhov[1,3], O. Rybdylova[4], S.S. Sazhin[4*]

[1] *Kutateladze Institute of Thermophysics, Novosibirsk, 630090, Russian Federation*

[2] *Novosibirsk State University, Novosibirsk, 630090, Russian Federation*

[3] *Novosibirsk State Technical University, Marx Ave., 20, Novosibirsk, 630073, Russian Federation*

[4] *Advanced Engineering Centre, University of Brighton, Brighton, BN2 4GJ, UK*

April 13, 2021

Abstract

The paper focuses on experimental investigation and modelling of the evaporation of supported ethanol/water droplets in an air flow. The modelling is based on the effective thermal conductivity/effective diffusivity model, using the analytical solutions to the transient heat transfer and species diffusion equations in droplets at each time step. The contribution of the supporting thread is included in the model. Model predictions are shown to be compatible with experimental data. For all mass fractions of ethanol, droplet surface temperatures rapidly decrease initially. This is followed by an increase in this temperature for non-zero mass fractions of ethanol in the mixture. For pure water this temperature remains almost constant after an initial decrease. In all cases, droplet diameters to power 1.5 decrease almost linearly with time. This agrees with model predictions in the limit for large droplet Reynolds numbers.

Keywords:
droplets, evaporation, forced convection, ethanol-water solution, effect of support

*Corresponding author: S.Sazhin@brighton.ac.uk

Nomenclature

a_d	equatorial radius of the spheroid [m]
B_T	Spalding heat transfer number [-]
c_d	distance from centre to pole [m] or specific heat capacity [J/(kg K)]
d	effective diameter [m]
d_t	diameter of the thread [m]
D	diffusion coefficient [m^2/s]
h	convective heat transfer coefficient [$W/(m^2\ K)$]
k	thermal conductivity [W/(m K)]
L	heat of evaporation [J/(kg)]
$\dot{m}_d$	droplet evaporation rate [kg/s]
Nu	Nusselt number [-]
P	external heating source term [K/s]
Pr	Prandtle number [-]
R	distance from the droplet centre [m]
R_d	droplet radius [m]
Re	Reynolds number [-]
S_C	contact area of the droplet with the thread [m^2]
Sh	Sherwood number [-]
t	time [s]
T	temperature [K]
v	velocity [m/s]
Y	mass fraction [-]

Greek symbols

β_c	coefficient in the Ranz and Marchall model [-]
ε	parameter determined by Expression (6) [-]
κ	thermal diffusivity [m^2/s]
ν	kinematic viscosity [m^2/s]
ρ	density [kg/m^3]

Subscripts

d	droplet
eff	effective
g	gas
i	liquid components
l	liquid

p	constant pressure
s	surface
v	vapour
0	initial condition

1. Introduction

Investigation of droplet evaporation in a gaseous environment is known to be important for various engineering applications [1, 2]. Despite the importance of these applications, there are many aspects of droplet evaporation processes which are still not well understood [3]. The problem becomes even more complex for multicomponent droplets [3].

Experimental investigations of the evaporation of multicomponent droplets are described in many papers, including [4, 5, 6]. The analysis of the approaches and the results presented in these and similar papers is not presented this paper. Our focus will be on investigation of the evaporation of water/ethanol droplets. The investigation of these droplets has been rather limited despite their importance for various applications. Among these applications is surface cooling by a water-ethanol mixture [7, 8, 9].

To control this and similar processes it is important to understand the details of evaporation of an isolated water/ethanol droplet in a wide range of gas flow parameters and droplet compositions. Among few available examples of such studies we can mention [10], where the results of the experimental investigation referring to sessile water/ethanol droplets are described. More recently, a similar problem but for droplets on an inclined surface was investigated by the authors of [11, 12]. The authors of [13] compared the experimentally observed evaporation characteristics of sessile and suspended water/ethanol droplets. The results of experimental investigation of the evaporation of supported water/ethanol droplets are presented in [14].

The current paper is primarily focused on linking the experimental results presented in [14] and the modelling approach developed at the University of Brighton [3]. An overview of the experimental setup and procedure is given in Section 2. The models to be used for the analysis of experimental data are presented and discussed in Section 3. A comparison between the experimental and modelling results is presented in Section 4. The most important results of the paper are presented in Section 5.

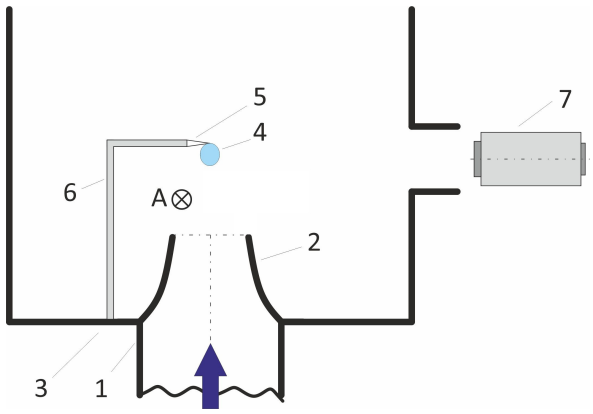

Figure 1: Schematic diagram of the experimental setup. 1 – honeycomb; 2 – narrowed channel; 3 – protective cover; 4 – droplet; 5 – suspension thread; 6 – holder; 7 – thermal image/video camera; A – point of measurement of velocity/temperature/humidity of gas flow.

2. Experimental setup and procedure

A description of the experimental results and procedure are presented in [14]. In what follows, these will be briefly summarised.

The setup used in our experiments is schematically shown in Figure 1. The droplets were suspended on an asbestos thread with diameter 0.3 mm[1] and k =0.15 W/(m K) [15]. The experiments were performed in a dry air flow with velocities 1 – 3 m/s and temperatures 26°C – 29°C.

Gas was supplied from a compressed air vessel into a cylindrical heating section with a diameter of 150 mm. Then the gas was passed through a narrowed channel (diameter 60 mm), the top part of which is shown in Figure 1. To reduce disturbances to the flow two honeycombs with mesh sizes of 0.5 mm and 0.2 mm, and spaced 380 mm apart, were installed in this channel. The top honeycomb is shown as '1' in Figure 1. For additional smoothing of the flow a narrowed channel was installed with a top diameter of 12 mm (see '2' in Figure 1). The distance between the droplet holder (see '5' in Figure 1) and the top of the narrowed channel was 20 mm.

A digital microscope (Digi Scope II v3) and a thermal imaging camera (NEC TH7102IR) with macro-objective TH 71-377 were used to determine the droplet sizes and surface temperatures in the experiments (see '7' in

[1]Note a typo in [14] where this diameter is described equal to 0.1 mm.

Figure 1). The camera worked in the spectral wave length range 8-14 μm. At these wave lengths the depth of penetration of infrared radiation in water did not exceed 9 μm which determines the maximal thickness of the near-surface region of the droplet in which the temperature was measured. The measurement errors did not exceed 0.2 K. Temperature measurements were taken every 5 s. A more detailed analysis of the methodology used in this part of our experiments is described in [16]-[20].

A hygrometer (Model 872) was used to determine the relative humidity of the air with errors of about 4%. Ethanol/water solutions (mass fractions of ethanol in the range 0 – 94%) were used. The errors of droplet radii and surface temperature measurements were about 50 μm and 0.08 K, respectively.

The initial droplet diameters were close to 2 mm (precise values will be identified for specific experiments), and their initial temperatures T_0 were the same as the ambient temperatures. Air humidity was close to zero. Approximating droplets as spheroids, their effective diameters d were estimated as: $d = (a_d^2 c_d)^{1/3}$, where a_d is the equatorial radius of the spheroid, and c_d the distance from centre to pole along the axis of symmetry. The measurements were performed up to $d = 0.3 d_0$ by which time about 97% of the volume of each droplet evaporated.

3. Models and approximations

The model suggested by Abramzon and Sirignano [21] was used for the investigation of the processes in the ambient gas.

The processes inside the droplet were modelled based upon the heat transfer and species diffusion equations assuming that these processes are spherically symmetric [1]:

$$\frac{\partial T}{\partial t} = \kappa_{\text{eff}} \left(\frac{\partial^2 T}{\partial R^2} + \frac{2}{R} \frac{\partial T}{\partial R} \right) + P, \tag{1}$$

$$\frac{\partial Y_{li}}{\partial t} = D_{\text{eff}} \left(\frac{\partial^2 Y_{li}}{\partial R^2} + \frac{2}{R} \frac{\partial Y_{li}}{\partial R} \right), \tag{2}$$

where $T \equiv T(R,t)$ and $Y_{li} \equiv Y_{li}(R,t)$ are the temperature and mass fraction of species $_i$ inside droplets, R and t are the distance from the droplet centre and time, respectively, κ_{eff} and D_{eff} are effective thermal and species diffusivity, respectively. These diffusivities take into account the effects of

recirculation inside droplets due to their motion relative to the gas, using the Effective Thermal Conductivity (ETC) and Effective Diffusivity (ED) models (see [1] for the details). $P \equiv P(R,t)$ accounts for the effects of external heating inside droplets (e.g. thermal radiation).

Equations (1) and (2) were solved analytically assuming that $T(R,t)$ and $Y_{li}(R,t)$ are twice continuously differentiable functions in the domain $0 \leq R \leq R_d$ (R_d is droplet radius), using standard initial conditions and the following conditions at the droplet surface:

$$h(T_g - T_{\text{eff}}) = k_{\text{eff}} \left.\frac{\partial T}{\partial R}\right|_{R=R_d-0}, \tag{3}$$

$$\left.\frac{\partial Y_{li}}{\partial R}\right|_{R=R_d-0} = \frac{\dot{m}_d}{4\pi R_d^2 D_{\text{eff}} \rho_l} \left(Y_{li} - \varepsilon_i\right). \tag{4}$$

where

$$T_{\text{eff}} = T_g + \frac{\rho_l L \dot{R}_d}{h}, \tag{5}$$

$$\varepsilon_i = \frac{Y_{vis}}{\sum_i Y_{vis}}, \tag{6}$$

$$\dot{R}_d = \frac{\dot{m}_d}{4\pi R_d^2 \rho_l}, \tag{7}$$

h and $\dot{m}_d$ are the convection heat transfer coefficient and the rate of droplet evaporation, respectively, k_{eff} is the effective thermal conductivity (used in the Effective Thermal Conductivity model), ρ_l and L are liquid density and specific heat of evaporation, respectively.

The explicit expressions for these analytical solutions in the form of a quickly converging series are given in [1]. They were implemented into the numerical code and used at every time step for calculations of droplet heating and evaporation [1, 3]. This allowed us to fully take into account the dependence of all input parameters on time and temperature. The advantages of this approach compared with the one based on a purely numerical solution to Equations (1) and (2) are discussed in [1, 3].

Note that in many approaches to the modelling of droplet heating and evaporation, including the most recent ones [22, 23], it was assumed that the gradients of temperature and species mass fractions inside the droplets can be ignored. This approach can be justified in many cases at the late stages

of droplet evaporation but should be used with care at the initial stages of the process [1, 3].

The effect of thermal expansion was modeled as in [1]. It is assumed that droplets are spherical, although it is applicable to spheroidal droplets with small eccentricities. As shown in [24], the evaporation times of spheroidal and spherical droplets are close when the eccentricity of the former does not exceed 1.5. Following [21], the Clift et al. approximations [25] (see Expressions (21) in [21]) were used to describe the dependence of Nu and Sh on Re (see Formula (9)).

The contribution of the supporting thread was accounted for using the approach developed in [26]. In this approach, the analytical solution to the transient heat transfer equation inside a semi-transparent droplet in the presence of thermal radiation was used to estimate heat transferred to the droplet via the supporting thread [1, 26]. It was assumed that this heat is instantaneously distributed in the whole volume of the droplet. This assumption is justified by the fact that the contribution of heat transferred to the droplet through the thread is much smaller than that of the ambient gas. This allowed us to use the analytical solution to the transient heat transfer equation with the thermal radiation to analyse droplet heating via the supporting thread. When applying this model we assumed, following [26], that the contact area of the droplet with the thread can be estimated as $S_c = \pi d_t R_d$, where d_t is the diameter of the thread, R_d is droplet radius.

Our analysis was based on Raoult's law [1]. Standard mixing laws, including Wilke's model for gas mixture,were used in our analysis, as in [27, 28]. Properties of individual components were taken from [27, 29, 30]. The ideal gas law was used.

The numerical details were essentially the same as used in [31, 32]. 500 equally distributed layers along droplet radii were used in calculations. 50 eigenvalues (terms in the series in the analytical solution) were used in both temperature and species mass fraction calculations. The introduction of layers inside the droplet is required for calculations of the integrals used in the analytical solution.

As shown in Table 1 of [31], the predictions of the model depend on the number of layers used in calculations when this number is less than 50 but do not change when this number increases to between 50 and 500. Since the conditions of our experiments are different from the setup analysed in [31], we used 500 layers in our analysis to mitigate this effect (we were not concerned about the computational cost at this stage). As follows from Figure 4 of [32],

using 10 eigenvalues leads to unacceptably large errors when predicting the values of mass fractions of the components near the centre and the surface of the droplets. At the same time using 40 eigenvalues led to reasonably accurate predictions of these mass fractions within the whole volume of the droplet. This justifies the decision to use 50 eigenvalues in our analysis.

The model used in our analysis is simplified if we assume that the droplet surface temperature does not change with time (we ignore the initial heat-up period). In this case all heat supplied from the gas is spent on droplet evaporation, which leads to the following expression for the derivative of the droplet radius:

$$\dot{R}_d = -\frac{k_g(T_g - T_s)}{2L\rho_l R_d}\mathrm{Nu}, \tag{8}$$

where the Nusselt number is estimated as [21, 25]:

$$\mathrm{Nu} = \left[1 + (1 + \mathrm{Re}\,\mathrm{Pr})^{1/3} f_c(\mathrm{Re})\right] \frac{1 + B_T}{B_T}, \tag{9}$$

$f_c(\mathrm{Re}) = 1$ at $\mathrm{Re} \leq 1$ and $f_c(\mathrm{Re}) = \mathrm{Re}^{0.077}$ at $1 < \mathrm{Re} \leq 400$, B_T is the Spalding heat transfer number

$$B_T = \frac{c_{pv}(T_g - T_s)}{L}, \tag{10}$$

c_{pv} is the specific heat capacity of vapour, Re and Pr are Reynolds (based on droplet diameter) and Prandtle numbers, respectively. When deriving (10) we took into account that no heat is spent on raising the droplet temperature.

In the limit of small Re, (9) is simplified to:

$$\mathrm{Nu} = 2\frac{\ln(1 + B_T)}{B_T}, \tag{11}$$

and the solution to (8) can be presented as

$$R_d^2 = R_{d0}^2 - \left[\frac{2k_g(T_g - T_s)}{L\rho_l}\frac{\ln(1 + B_T)}{B_T}\right] t. \tag{12}$$

This is a well known d^2 law [1].

In the limit of large Re (but $\mathrm{Re} < 400$), (9) is simplified to:

$$\mathrm{Nu} = \mathrm{Re}^{0.4}\mathrm{Pr}^{1/3}\frac{\ln(1 + B_T)}{B_T}. \tag{13}$$

In this case, the solution to (8) can be presented as:

$$R_d^{1.6} = R_{d0}^{1.6} - \left[\frac{0.8 k_g (T_g - T_s)}{L \rho_l} \left(\frac{2 v_d}{\nu_g} \right)^{0.4} \mathrm{Pr}^{1/3} \frac{\ln(1 + B_T)}{B_T} \right] t. \qquad (14)$$

This is the analogue of the d^2 law for large Re. Note that if we used not the Clift et al. correlation for Nu [21, 25] but the one suggested by Ranz and Marchall (see [33] for in-depth analysis of this correlation), predicting that Nu is proportional to $\mathrm{Re}^{1/2}$, then Solution (14) would need to be replaced with the following solution:

$$R_d^{1.5} = R_{d0}^{1.5} - \left[\beta_c \frac{0.75 k_g (T_g - T_s)}{L \rho_l} \left(\frac{2 v_d}{\nu_g} \right)^{0.5} \mathrm{Pr}^{1/3} \frac{\ln(1 + B_T)}{B_T} \right] t, \qquad (15)$$

where coefficient β_c is commonly assumed equal to 0.6 [1]. Note that qualitative analysis of Nu at large Re, assuming a laminar boundary layer, supports proportionality of Nu to $\mathrm{Re}^{1/2}$ [34], although strong arguments to support the Clift et al. approximation were presented in [21]. We believe that Terekhov et al. [35] were the first to draw attention to this $d^{1.5}$ law.

Note that our calculations are based on the general formula (9) without any approximations for small or large values of Re and without any additional assumptions regarding the value of droplet surface temperature apart from Condition (3).

4. Modelling versus experimental data

In what follows some experimental results, obtained using the setup shown in Figure 1 and described in Section 2, and the results of the application of the models described in Section 3 are compared.

The focus of our analysis will be on droplet surface temperatures (T_s) and their diameters (d). Since all experiments were performed for droplets with initial temperatures equal to the ambient gas temperatures (T_g) which remained constant during the experiments, we will present the results for $T_g - T_s$ rather than for T_s. This approach will allow us to show more clearly the conditions in which droplet heating/cooling and evaporation takes place. Remembering that in all cases in our experiments the droplet Reynolds numbers (Re) are greater than 100 (but less than 400), we can expect Expressions (14) and (15) to be valid during most of the droplet heating and evaporation

period (except the initial heat-up period). Note that these expressions are not used in our analysis, although our results are close to the predictions of these formulae for large Re, as expected.

Remembering (15), following [35], our analysis will focus on $(d/d_0)^{1.5}$, where d_0 is the initial droplet diameter, rather than on d/d_0 or $(d/d_0)^2$, when studying the droplet evaporation process.

The plots of the experimentally observed and predicted values of $T_g - T_s$ of water droplets versus time are presented in Figure 2. As can be seen from this figure, for all gas velocities the observed $T_g - T_s$ initially rises very quickly and then stays at about the same level of around 15 K. Rather similar behaviours of $T_g - T_s$ are predicted by both models, taking into account and ignoring the contribution of the thread. The values predicted by the model in which the effects of the thread are taken into account are visibly closer to the experimental data than those predicted by the model ignoring this effect. The predictions of the latter model are about the same for all gas velocities. The model in which the contribution of the thread is taken into account predicts slight decreases in T_s after t greater than about 50 s; this is attributed to a reduction in droplet sizes due to evaporation, which is not clearly visible in the experimental data.

The time evolutions of experimentally observed and predicted values of the normalised droplet diameters $(d/d_0)^{1.5}$, for the same input parameters as in Figure 2, are shown in Figure 3. As mentioned earlier, for the conditions of our experiments $(d/d_0)^{1.5}$ is expected to be a linear function of time except at the initial heat-up stage (see Expression (15)).

As can be seen in Figure 3, both observed and predicted values of $(d/d_0)^{1.5}$ decrease almost linearly with time, as expected. The rate of this decrease visibly increases when flow velocity increases, from 1 m/s to 1.5 m/s, which was also expected. No clear decrease in this rate was seen in our experiments when air velocity was further increased. In all cases, the contribution of the initial heat-up stage can be ignored. As in the case shown in Figure 2, the model which takes into account the effect of the thread predicts $(d/d_0)^{1.5}$ that are much closer to those observed experimentally than does the model not taking into account this effect. Note that the predicted values of $(d/d_0)^{1.5}$ tend to be larger than those observed experimentally, especially for larger

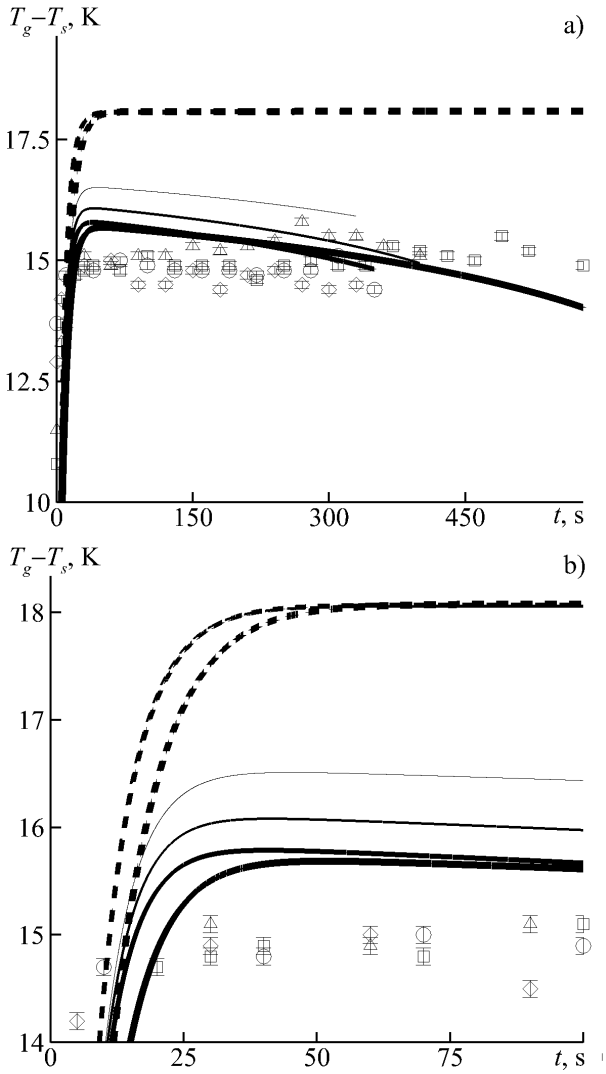

Figure 2: **(a)** $T_g - T_s$ for pure water versus time. Symbols refer to experimental data (Case 1 (squares): gas velocity 1 m/s, initial droplet diameter 2.47 mm; Case 2 (circles): gas velocity 1.5 m/s, initial droplet diameter 2.31 mm; Case 3 (triangles): gas velocity 2 m/s, initial droplet diameter 2.42 mm; Case 4 (diamonds): gas velocity 3 m/s, initial droplet diameter 2.67 mm; gas and initial droplet temperatures were 299 K in all cases). Solid (dashed) curves refer to predictions of the models for the same values of input parameters taking into account (ignoring) the effect of the thread. The thickest (thinnest) curves refer to Case 1(4). **(b)** Zoomed part referring to the initial stage of the process.

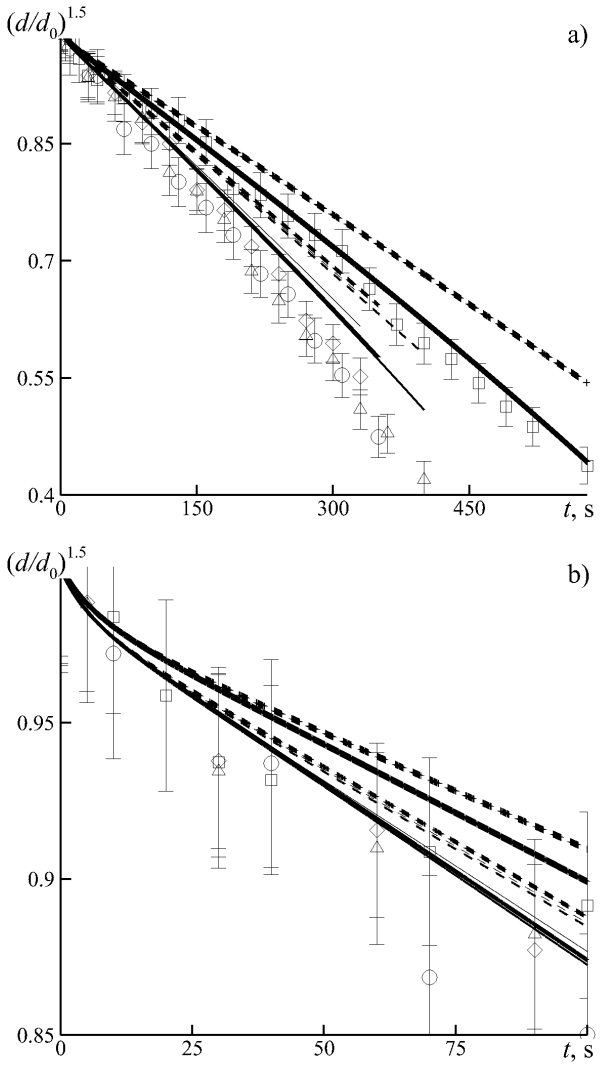

Figure 3: The same as Figure 2, but for $(d/d_0)^{1.5}$.

values of air velocity. Note the rather large error bars for the results shown in Figure 3.

The plots of the experimentally observed and predicted values of $T_g - T_s$ for water/ethanol droplets are presented in Figure 4. As can be seen from Figure 4, the addition of ethanol leads to a qualitative change in the function $T_g - T_s$. As in the case of water droplets, $T_g - T_s$ rapidly increases initially. In contrast to pure water droplets, however, this increase is followed by a decrease in $T_g - T_s$ for water/ethanol droplets. The minimal surface temperatures of water/ethanol droplets were always less than those of water droplets. The values of these minimal temperatures decrease as the mass fraction of ethanol increases.

Similarly to pure water droplets, the predictions of the model in which the contribution of the thread is taken into account are always closer to experimental data than those of the model in which it is ignored. In fact, the modelling and experimental results are closer for the water/ethanol droplets than for pure water droplets. Maximal deviations between observed and modelling results are seen for the mixture with 94% ethanol. Even in this case this deviation was only about 2 K.

Plots similar to those presented in Figure 3, but for water/ethanol droplets, are presented in Figure 5. As one can see from the latter figure, as in the case of pure water droplets, in all cases the values of $(d/d_0)^{1.5}$ decrease almost linearly with time. The rate of this decrease increases when the mass fraction of ethanol increases. This is in full agreement with the model predictions. In contrast to the cases shown in the previous figures, however, the improvement in the predictions of the model when the effects of the thread are considered is less clear. This improvement can be seen when ethanol is present in the mixture, but is not seen for pure water. Note that Case 1, shown in Figure 5, differs from Case 2, shown in Figure 3, in terms of the values of initial droplet diameter and ambient/droplet temperature.

In Figure 6, the results presented in Figure 5 for Case 2 are reproduced in three formats: (d/d_0) versus time, $(d/d_0)^{1.5}$ versus time and $(d/d_0)^2$ versus

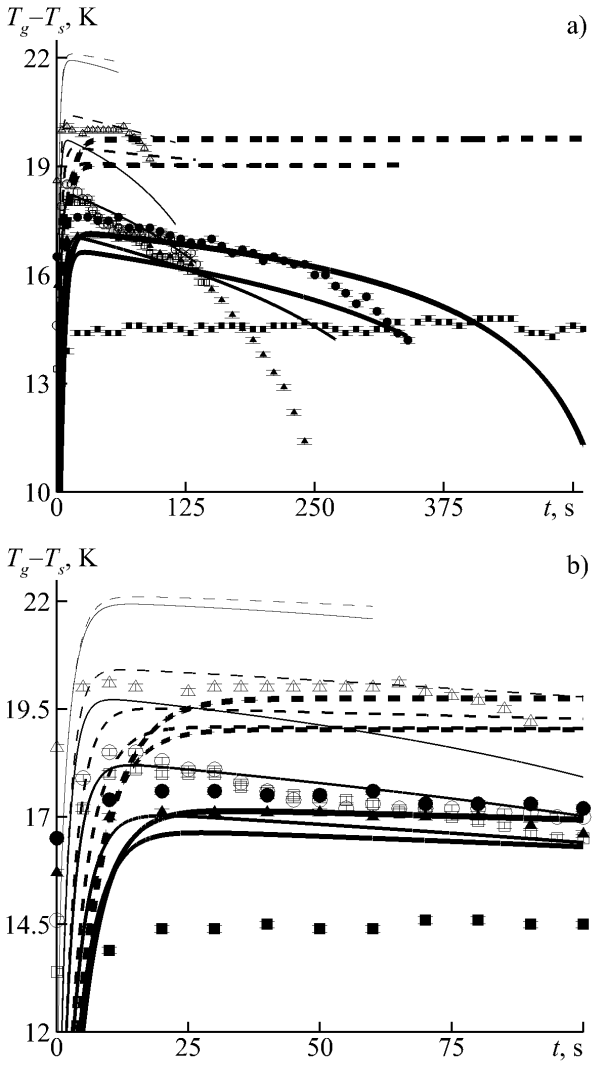

Figure 4: **(a)** $T_g - T_s$ for water/ethanol droplets versus time. Symbols refer to experimental data (Case 1 (filled squares): pure water, initial droplet diameter 2.15 mm; Case 2 (filled circles): mixture with mass fraction of ethanol 9%, initial droplet diameter 2.06 mm; Case 3 (filled triangles): mixture with mass fraction of ethanol 23%, initial droplet diameter 1.95 mm; Case 4 (empty squares): mixture with mass fraction of ethanol 47%, initial droplet diameter 1.87 mm; Case 5 (empty circles): mixture with mass fraction of ethanol 70%, initial droplet diameter 1.77 mm; Case 6 (empty triangles): mixture with mass fraction of ethanol 94%, initial droplet diameter 1.82 mm; in all cases gas velocity was 1.5 m/s and gas and initial droplet temperatures were 302 K). Solid (dashed) curves refer to predictions of the models for the same values of input parameters taking into account (ignoring) the effect of the thread. The thickest (thinnest) curves refer to Case 1(6). **(b)** Zoomed part referring to the initial stage of the process. Note that we halved the number of experimental point shown in part (a) to improve the presentation of the results.

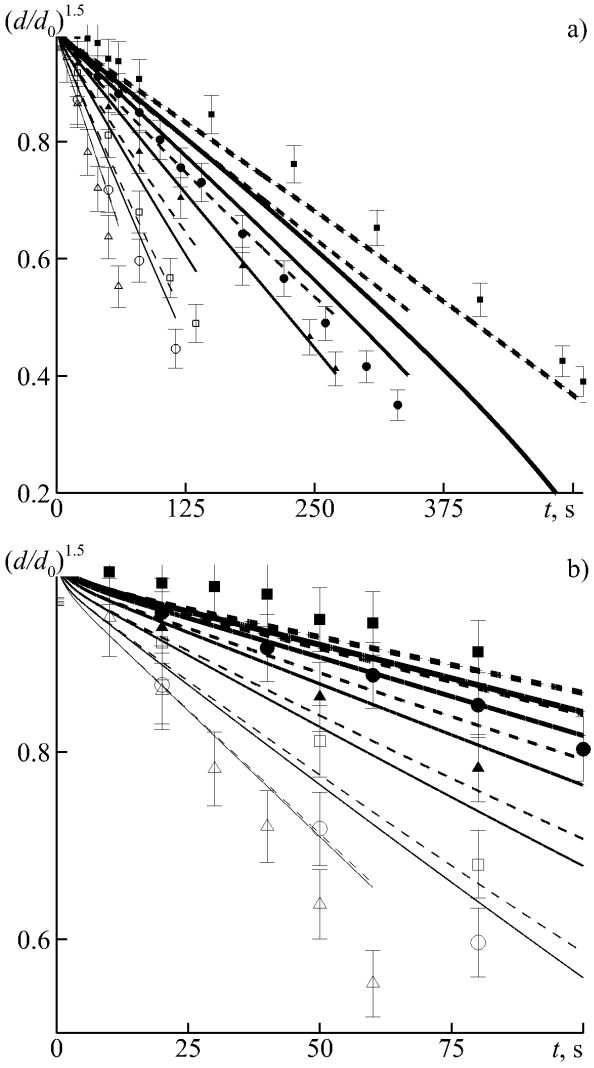

Figure 5: The same as Figure 4, but for $(d/d_0)^{1.5}$.

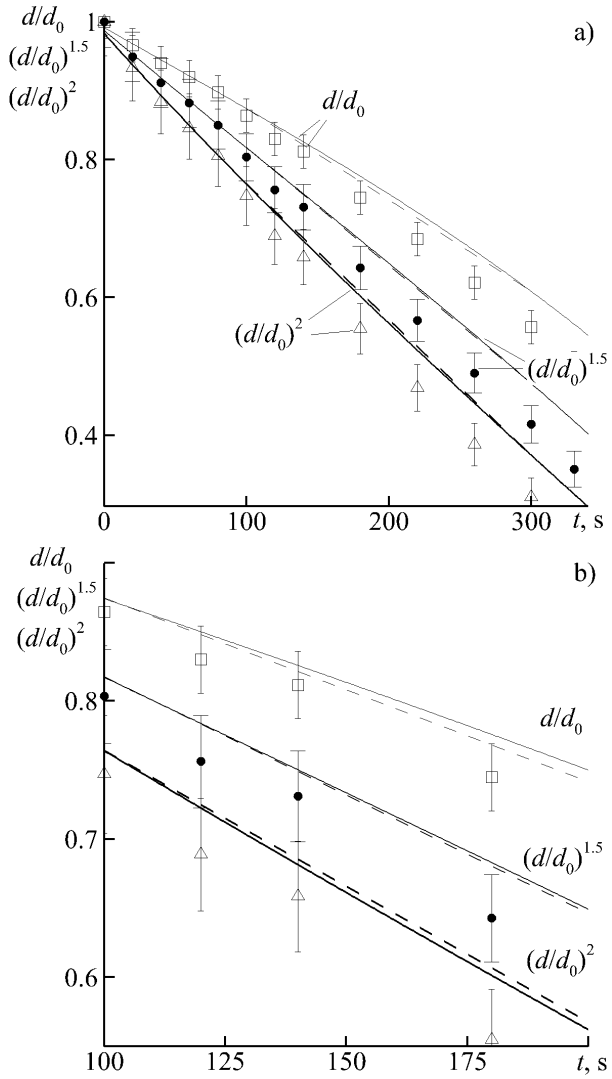

Figure 6: **(a)** The plots of (d/d_0), $(d/d_0)^{1.5}$ and $(d/d_0)^2$ for water/ethanol droplets versus time predicted by the model taking into account the effect of support for Case 2 (mixture with mass fraction of ethanol 9%, initial droplet diameter 2.06 mm). Symbols refer to experimental data. Dashed lines connect the predictions of the model at $t = 100$ s and $t = 300$ s; **(b)** Zoomed part referring to the time range 100 s to 200 s.

time. The dashed straight lines in this figure connect the predictions of the model at $t = 100$ s and $t = 300$ s. As can be seen from this figure, the predictions of the model are closest to the straight line for the plot of $(d/d_0)^{1.5}$ versus time which justifies our presentation of the results in this format in Figures 3 and 5. Time instant $t = 100$ s was chosen to ensure that the initial heat-up period is excluded from our analysis. In Figure 6, a small deviation of the curve for $(d/d_0)^{1.5}$ versus time from the straight line can be partly attributed to the fact that we approximated Nu using Formula (9). This formula predicts that $(d/d_0)^{1.6}$ versus time rather than $(d/d_0)^{1.5}$ versus time should be a straight line after the completion of the heat-up period.

5. Conclusions

Evaporation of suspended ethanol/water droplets, with various mass fractions of ethanol and water, in an ambient air flow is investigated experimentally. It is shown that in all cases droplet surface temperatures rapidly decrease initially. This is followed by an increase in these temperatures for non-zero mass fractions of ethanol in the mixture. For pure water this temperature remains almost constant after an initial decrease. In all cases droplet diameters to power 1.5 are shown to decrease almost linearly with time. This agrees with model predictions in the limit for large droplet Reynolds numbers.

These experimental results are shown to be compatible with the predictions of the model taking into account the effects of recirculation inside droplets, based on the effective thermal conductivity/effective diffusivity model and using the analytical solutions to the transient heat transfer and species diffusion equations in the liquid phase at each time step. The contribution of a supporting thread is taken into account using the analytical solution to the transient heat conduction equation in a spherical semi-transparent droplet in the presence of thermal radiation. The heat supplied to the droplet via the supporting thread was found following the same procedure used to find the thermal radiation energy absorbed inside the droplet. It is assumed that heat supplied via this thread is instantaneously and homogeneously distributed throughout the whole volume of the droplet. In most cases considered in our experiments, taking into account the contribution of the supporting thread leads to visible improvements in the predictions of the model.

Acknowledgements

Work on this paper was supported by the Russian Foundation for Fundamental Research (grant no. 20-58-10003KO_a) (contributions by E.M. Starinskaya, N.B. Miskiv, A.D. Nazarov, V.V. Terekhov, and V.I. Terekhov), the Royal Society (UK) (Grant no. IEC 192007) (contributions by O. Rybdylova and S.S. Sazhin), and the EPSRC (Grant no. MR/T043326/1) (contribution by O. Rybdylova).

References

[1] S.S. Sazhin, Droplets and Sprays. Springer (2014).

[2] A.Y. Varaksin, Fluid dynamics and thermal physics of two-phase flows: Problems and achievements, High Temperature 51 (2013) 377-407.

[3] S.S. Sazhin, Modelling of fuel droplet heating and evaporation: Recent results and unsolved problems, Fuel 196 (2017) 69-101.

[4] G. Brenn, L.J. Deviprasath, F. Durst, F., C. Fink, Evaporation of acoustically levitated multi-component liquid droplets, Int. J. Heat Mass Transf. 50 (2007) 5073-5086.

[5] C. Maqua, G. Castanet, F. Grisch, F. Lemoine, T. Kristyadi, S.S. Sazhin, Monodisperse droplet heating and evaporation: experimental study and modelling, Int. J of Heat and Mass Transf. 51 (2008) 3932-3945.

[6] T. Kristyadi, V. Depredurand, G. Castanet, F. Lemoine, S.S. Sazhin, A. Elwardany, E.M. Sazhina E.M., M.R. Heikal, Monodisperse monocomponent fuel droplet heating and evaporation, Fuel 89 (2010) 3995-4001.

[7] P.N. Karpov, A.D. Nazarov, A.F. Serov, V.I. Terekhov, Evaporative cooling by a pulsed jets spray of binary ethanol-water mixture, Techn. Phys. Lett., 41 (2015) 668-671.

[8] H. Liu, C. Cai, H. Yin, J. Luo, M. Jia, J. Gao, Experimental investigation on heat transfer of spray cooling with the mixture of ethanol and water, Int. J. of Thermal Sciences 133 (2018) 62-68.

[9] V.I. Terekhov, P.N. Karpov, A.D. Nazarov, A.F. Serov, Unsteady heat transfer at impinging of a single spray pulse with various durations, Int. J. Heat Mass Transf. 158 (2020) 120057. .

[10] K. Sefiane, L. Tadrist, M. Douglas, Experimental study of evaporating water/ethanol mixture sessile drop: influence of concentration, Int. J. of Heat and Mass Transf. 46 (2003) 4527-4534.

[11] Y. Yonemoto, S. Suzuki, S. Uenomachi, T. Kunugi, Sliding behaviour of water-ethanol mixture droplets on inclined low- surface-energy solid, Int. J. Heat and Mass Transf. 120 (2018) 1315-1324

[12] P. Katre, P. Gurrala, S. Balusamy, S. Banerjee, K.C. Sahu, Evaporation of sessile ethanol-water droplets on a critically inclined heated surface, Int. J. Multiphase Flow 131 (2020) 103368.

[13] V.Y. Borodulin, V.N. Letushko, M.I. Nizovtsev, A.N. Sterlyagov, The experimental study of evaporation of water–alcohol solution droplets. Colloid. J. 81 (2019) 219–225.

[14] E.M. Bochkareva, N.B. Miskiv, A.D. Nazarov, V.V. Terekhov, V.I. Terekhov, Exprimental study of evaporating droplets suspended ethanol-water solution under conditions of forced convection. Interfacial Phenomena and Heat Transfer, 6(2) (2018) 115-127.

[15] N.B. Vagraftik, Handbook of Thermophysical Properties of Fluids. Stars Publishing House, Moscow (2006) (in Russian).

[16] L. Tarozzi, A. Muscio, P. Tartarini, Experimental tests of dropwise cooling on infrared-transparent media, Exp. Therm. Fluid Sci. 31 (2007) 857–865.

[17] P. Tartarini, M.A. Corticelli, L. Tarozzi, Dropwise cooling: experimental tests by infrared thermography and numerical simulations, Appl. Therm. Eng. 29 (2009) 1391–1397.

[18] T.A. Yakhno, O.A. Sanina, A.G. Sanin, V.G. Yakhno, M.G. Volovik, Thermographic investigation of the temperature field dynamics at the liquid-air interface in drops of water solutions drying on a glass substrate, Technical Physics, Russian J. Appl. Phys. 7 (2012) 915–922.

[19] A.A. Fedorets, L.A. Dombrovsky, A.M. Smirnov, The use of infrared self-emission measurements to retrieve surface temperature of levitating water droplets, Infrared Phys. Technol. 69 (2015) 238–243.

[20] V.Yu. Borodulin, V.N. Letushko, M.I. Nizovtsev, A.N. Sterlyagov, Determination of parameters of heat and mass transfer in evaporating drops, Int. J Heat and Mass Transfer 109 (2017) 609-618.

[21] B. Abramzon, W.A. Sirignano, Droplet vaporization model for spray combustion calculations, Int. J Heat Mass Transfer 32 (1989) 1605-1618.

[22] A.P. Pinheiro, J.M. Vedovoto, A.da S. Neto, B.G.M. van Wachem, Ethanol droplet evaporation: Effects of ambient temperature, pressure and fuel vapor concentration, Int. J Heat Mass Transfer 143 (2019) 118472.

[23] P. Narasu, S. Boschmann, P. Pöschko, F. Zhao, E. Gutheil, Modeling and simulation of single ethanol/water droplet evaporation in dry and humid air, Combustion Science and Technology (2020) https://doi.org/10.1080/00102202.2020.1724980

[24] V.S. Zubkov, G.E. Cossali, S. Tonini, O. Rybdylova, C. Crua, M. Heikal, S.S. Sazhin, Mathematical modelling of heating and evaporation of a spheroidal droplet, Int. J. Heat Mass Transf. 108 (2017) 2181-2190.

[25] R. Clift, J.R. Grace, M.E. Weber, Bubbles, Drops and Particles. New York, Academic Press (1978).

[26] P.A. Strizhak, R.S. Volkov, G. Castanet, F. Lemoine, O. Rybdylova, S.S. Sazhin, Heating and evaporation of suspended water droplets: Experimental studies and modelling, Int. J. Heat Mass Transf. 127 (2018) 92-106.

[27] B.E. Poling, J.M. Prausnitz, J.P. O'Connell, The Properties of Gases and Liquids, Fifth Edition, 2001.

[28] R.B. Bird, E.W. Stewart, E.N. Lightfoot, Transport Phenomena, second ed., Wiley & Sons, New York, Chichester, 2002.

[29] C.L. Yaws, editor, Thermophysical Properties of Chemicals and Hydrocarbons. William Andrew Inc., 2008.

[30] C.L. Yaws, editor, Transport Properties of Chemicals and Hydrocarbons: viscosity, thermal conductivity, and diffusivity of C1 to C100 organics and Ac to Zr Inorganics-William Andrew (2009)

[31] O. Rybdylova, M. Al Qubeissi, M. Braun, C. Crua, J. Manin, L.M. Pickett, G. de Sercey, E.M. Sazhina, S.S. Sazhin, M. Heikal, A model for droplet heating and its implementation into ANSYS Fluent, Int. Comm. Heat and Mass Transf. 76 (2016) 265-270.

[32] O. Rybdylova, L. Poulton, M. Al Qubeissi, A.E. Elwardany, C. Crua, T. Khan, S.S. Sazhin, A model for multi-component droplet heating and evaporation and its implementation into ANSYS Fluent, Int. Comm. Heat and Mass Transf. 90 (2018) 29-33.

[33] A. Aissa, M. Abdelouahab, A. Noureddine, M. El Ganaoui, B. Pateyron, Ranz and Marcshall correlations limits on heat flow between a sphere and its surrounding gas at high temperature. Therm. Sci. 19(5) (2015) 1521–1528.

[34] N.A. Fuchs, Evaporation and Droplet Growth in Gaseous Media. Pergamon Press, London (1959).

[35] V.I. Terekhov, V.V. Terekhov, N.E. Shishkin, K.Ch. Bi, Heat and mass transfer in disperse and porous media: investigation of non-stationary evaporation of liquid droplets, J. of Engineering Physics and Thermophysics 83(5) (2010) 883-890.